



# Calibrating 1D hydrodynamic river models in the absence of cross-sectional geometry: A new parameterization scheme

Liguang Jiang<sup>1,2</sup>, Silja Westphal Christensen<sup>2,3</sup>, Peter Bauer-Gottwein<sup>2</sup>

<sup>1</sup>School of Environmental Science and Engineering, Southern University of Science and Technology, Shenzhen, 518055, China

<sup>2</sup>Department of Environmental Engineering, Technical University of Denmark, 2800 Kgs. Lyngby, Denmark

<sup>3</sup>Department of Applied Mathematics and Computer Science, Technical University of Denmark, 2800 Kgs. Lyngby, Denmark

10 *Correspondence to:* Liguang Jiang (jianglg@sustech.edu.cn)

**Abstract.** Hydrodynamic modeling has been increasingly used to simulate water surface elevation which is important for flood prediction and risk assessment. Scarcity/inaccessibility of in-situ bathymetric information has hindered hydrodynamic model development at continental-global scales. Therefore, river cross-section geometry has commonly been approximated using highly simplified generic shapes. However, strong correlations appear between cross-section shape parameters and hydraulic roughness in a hydraulic inversion approach. This study introduces a novel parameterization of 1D hydrodynamic models that reduces ambiguity by combining cross-section geometry and roughness into a conveyance parameter. Flow area and conveyance are expressed as power-law functions of flow depth, and thus are assumed to be linearly related in log-log space at reach scale. Data from a wide range of river systems show that the linearity approximation is globally applicable. Because the two are expressed as power-law functions of flow depth, no further assumptions about channel geometry are needed. Therefore, the hydraulic inversion approach allows for calibrating flow area and conveyance curves in the absence of bathymetry and hydraulic roughness. Its feasibility and performance are illustrated using satellite observations of river width and water surface elevation.

## 1 Introduction

Hydrodynamic modeling of rivers is important for quantitative assessment of river flow and water level dynamics and, critically, for risk assessment and flood prediction. It has been widely used for many applications, such as estimates of hydraulic parameters (e.g. water surface elevation (WSE), longitudinal profile, velocity), flood forecasting, inundation estimation, risk assessment, river maintenance, etc. (Andreadis and Schumann, 2014; Bates et al., 2014; Bierkens, 2015; Blöschl et al., 2015; Jiang et al., 2020). Nowadays, in the era of big data, earth observation datasets, cloud computing, and complex modeling platforms are available for better simulations of WSE at different scales (Fleischmann et al., 2019; Gleason and Durand, 2020; Ward et al., 2015).



Traditional hydrodynamic modeling approaches require detailed river channel bathymetry, which is usually represented by cross-sectional geometry. There are, however, a limited number of rivers, for which the surveyed cross-sectional geometry is available. The challenge that arises in many studies is how to approximate the channel geometry. This is a common problem facing the scientific community. A common approach is to parameterize channel geometry as a simple shape, e.g. a rectangle or triangle (Garambois et al., 2017; Jiang et al., 2019; Neal et al., 2012; Schneider et al., 2017). Instead of rectangular or triangular shapes, Dingman (2007) and Neal et al. (2015) used a power function (bankfull width and depth are required) to represent channel shape variability between the limiting cases of rectangular and triangular shape. However, Neal et al. (2015) used a uniform shape instead of varying shapes along the channel. Similar parameterizations of cross section shapes were used in Mejia & Reed (2011), and the effect of assumed shapes on simulated flows was investigated. Some studies estimated river bathymetry using global DEMs combined with an assumed simplified shape (e.g. rectangle) of the submerged portion of the river. Domeneghetti (2016) used DEM data to infer the river bathymetry based on width-elevation relationships of high flow and low flow, respectively. Similarly, a few studies infer bathymetry from water surface height and width by fitting the relationship between the two. Obviously, the success of this approach depends on the channel exposure (Mersel et al., 2013). Moreover, combinations of remote sensing data and empirical statistical relationships or data assimilation approaches have also been used to infer effective bathymetry (Brisset et al., 2018; Dey et al., 2019; Durand et al., 2008; Fonstad and Marcus, 2005; Grimaldi et al., 2018; Larnier et al., 2020; Legleiter, 2015; Moramarco et al., 2019; Schaperow et al., 2019). For instance, Durand et al. (2008) estimated bathymetric depth and slope by assimilating synthetic WSE data from the Surface Water and Ocean Topography (SWOT) mission into the LISFLOOD-FP hydrodynamic model. Larnier et al. (2020) also applied data assimilation to infer effective bathymetry from synthetic SWOT altimetry measurements within an inverse framework. Here we do not comprehensively review bathymetry estimation using upcoming SWOT mission data. Instead, we refer the reader to Biancamaria et al. (2016) and Gleason & Durand (2020) for a broader overview.

In addition to the channel bathymetry, channel roughness is another factor that is important to simulate flow dynamics with sufficient accuracy (Bates et al., 2014; Neal et al., 2015). Usually, a uniform value is adopted to represent channel/floodplain roughness although large heterogeneity of river morphology exists in most cases (Annis et al., 2020; Jiang et al., 2020; Pappenberger et al., 2007; Schumann et al., 2007). When calibrating channel geometry parameters along with roughness parameters, strong parameter correlation appears between cross section shape (wetted perimeter) and hydraulic roughness. That is, roughness parameter will be “effective”, not only representing the friction but also compensating for inaccurate geometry, which affects the hydraulic resistance through the wetted perimeter. Therefore, roughness and geometry parameters trade-off against each other, which has been widely reported (see Garambois & Monnier (2015) and references therein).

In order to address this ambiguity in hydraulic inverse problems, we put forward a method to parameterize and calibrate the 1-D river models in a different way. Instead of roughness and geometry, flow area and conveyance curves as functions of



65 flow depth are estimated in an inverse modeling workflow. In this way, only the dependence of area and conveyance on flow depth is estimated, regardless of the detailed channel shape and roughness. This paper illustrates this approach for the calibration of an 1D MIKE Hydro River model (DHI, 2017) to simulate WSE dynamics, using satellite observations of WSE and river width.

## 2 Methods

### 2.1 Theoretical background

70 Flow in open channels can be described by the continuity equation and momentum equation, known as the de Saint-Venant equations (Chow, 1959):

$$\frac{\partial A(d)}{\partial t} + \frac{\partial Q}{\partial x} = 0 \quad (1)$$

$$\frac{\partial Q}{\partial t} + \frac{\partial}{\partial x} \left( \frac{Q^2}{A(d)} \right) + gA(d) \frac{\partial d}{\partial x} - gA(d)(S_0 - S_f) = 0 \quad (2)$$

75 where:  $A$  is the cross-sectional area;  $Q$  is the discharge;  $d$  is the flow depth;  $S_0$  is the slope of the channel bottom;  $S_f$  is the friction slope;  $g$  is the gravity acceleration;  $t$  is time and  $x$  is chainage, i.e. the distance along the channel.

Equations (1) and (2) compose the 1-D dynamic wave model. In the absence of cross-sectional geometry, there are five unknowns in this model, i.e.  $A$ ,  $Q$ ,  $d$ ,  $S_0$ , and  $S_f$ . To effect a solution of  $Q$  and  $d$ , information about channel geometry and friction slope is required. Flow area  $A$  and channel slope  $S_0$  can be obtained once bathymetry is known. Friction slope  $S_f$  can be approximated using the Manning formula or the Chézy formula (Chow, 1959).

80 Here, we express friction slope as a function of conveyance ( $K$ ) and discharge ( $Q$ ) using Manning's equation

$$Q = KS_f^{\frac{1}{2}} \quad (3)$$

$$K = \frac{1}{n} A R^{\frac{2}{3}} \quad (4)$$

where,  $n$  is the Manning roughness coefficient and  $R$  is the hydraulic radius. The conveyance is a measure of water carrying capacity of a cross section since it is directly proportional to discharge (Chow, 1959).

85 Substituting for  $S_f$ , the momentum equation is written as:

$$\underbrace{\frac{\partial Q}{\partial t} + \frac{\partial}{\partial x} \left( \frac{Q^2}{A(d)} \right)}_{\text{inertia terms}} + \underbrace{gA(d) \frac{\partial d}{\partial x} - gA(d) \left( S_0 - \frac{Q^2}{K^2(d)} \right)}_{\text{Kinematic wave}} = 0 \quad (5)$$

*Diffusive wave*

*Dynamic wave*



This version of the momentum equation (5) indicates that, in steady state (for both kinematic wave and diffusive wave),  $K(d)$  is much more sensitive than  $A(d)$ , and  $A(d)$  appears only when the flow accelerates or decelerates.

## 2.2 Parameterization of flow area and conveyance curves

- 90 Equations (1) and (5) provide two equations with still five unknowns, i.e.  $A$ ,  $Q$ ,  $d$ ,  $S_o$ , and  $K$ . However,  $K$  and  $A$  are related to flow depth,  $d$ . If  $K$  and  $A$  can be expressed as functions of  $d$ ,  $Q$  and  $d$  can be solved for, given the slope  $S_o$  but without the need for detailed information on cross-sectional shape and roughness. The hydraulic geometry relations are widely used to relate the water surface width, average depth, and average velocity to discharge since it was introduced by Leopold and Maddock in 1953 (Bjerklie et al., 2005; Dingman, 2007; Ferguson, 1986; C. J. Gleason, 2015; Leopold & Maddock, 1953).
- 95 Dingman (2007) has derived explicit equations for the exponent and coefficients in the power-law function, explaining the variation of hydraulic geometry in different rivers. In some way analogous to the at-a-station power-law of hydraulic geometry, power function relationships that relate flow area  $A$  and conveyance  $K$  to flow depth  $d$  of a cross section can be written, respectively, as (Chow, 1959; Garbrecht, 1990):

$$A(d) = a d^\beta \quad (6)$$

100  $K(d) = c d^\delta \quad (7)$

$$d = H - Z_0 \quad (8)$$

where,  $a$ ,  $\beta$ ,  $c$  and  $\delta$  are empirical coefficients;  $H$  and  $Z$  are WSE and channel datum, i.e. water surface elevation for zero flow.

Transforming equations (6) and (7) into log-log space, we can write the following linear relationships:

105  $\log A(x, t) = \alpha(x) + \beta(x) \log d(x, t) \quad (9)$

$$\log K(x, t) = \gamma(x) + \delta(x) \log d(x, t) \quad (10)$$

- where  $\alpha = \log(a)$  and  $\gamma = \log(c)$ . This relationship is investigated for different rivers having a wide range of river width (three orders of magnitude) to show its validity for real-world rivers. Note that, these six rivers are used simply due to the availability of cross-section data (see a map of rivers in Fig. S1). Strong positive linear relationships are readily revealed by plotting the logarithmic  $A \sim d$ , and  $K \sim d$  pairs for any given cross section below bankfull depth (Figure 1). A discontinuity may occur if significant flood plain exists as the case of the Yellow River (Figure 1d). Chow (1959) and Garbrecht (1990) suggested using separate functions to approximate the hydraulic properties below and above bankfull depth. In this initial study, one single power-law function is used. Note that the conveyance changes with the Manning's number, but the linear relationship holds (Fig. S2). To calculate conveyance, spatially varying, randomly distributed Manning's number ranging between 0.015 and 0.05 are used to mimic real-world rivers instead of unrealistic uniform values along the whole reach. A uniform Manning's number results in a much stronger linear relationship (Figures S2 and S3).
- 110
- 115

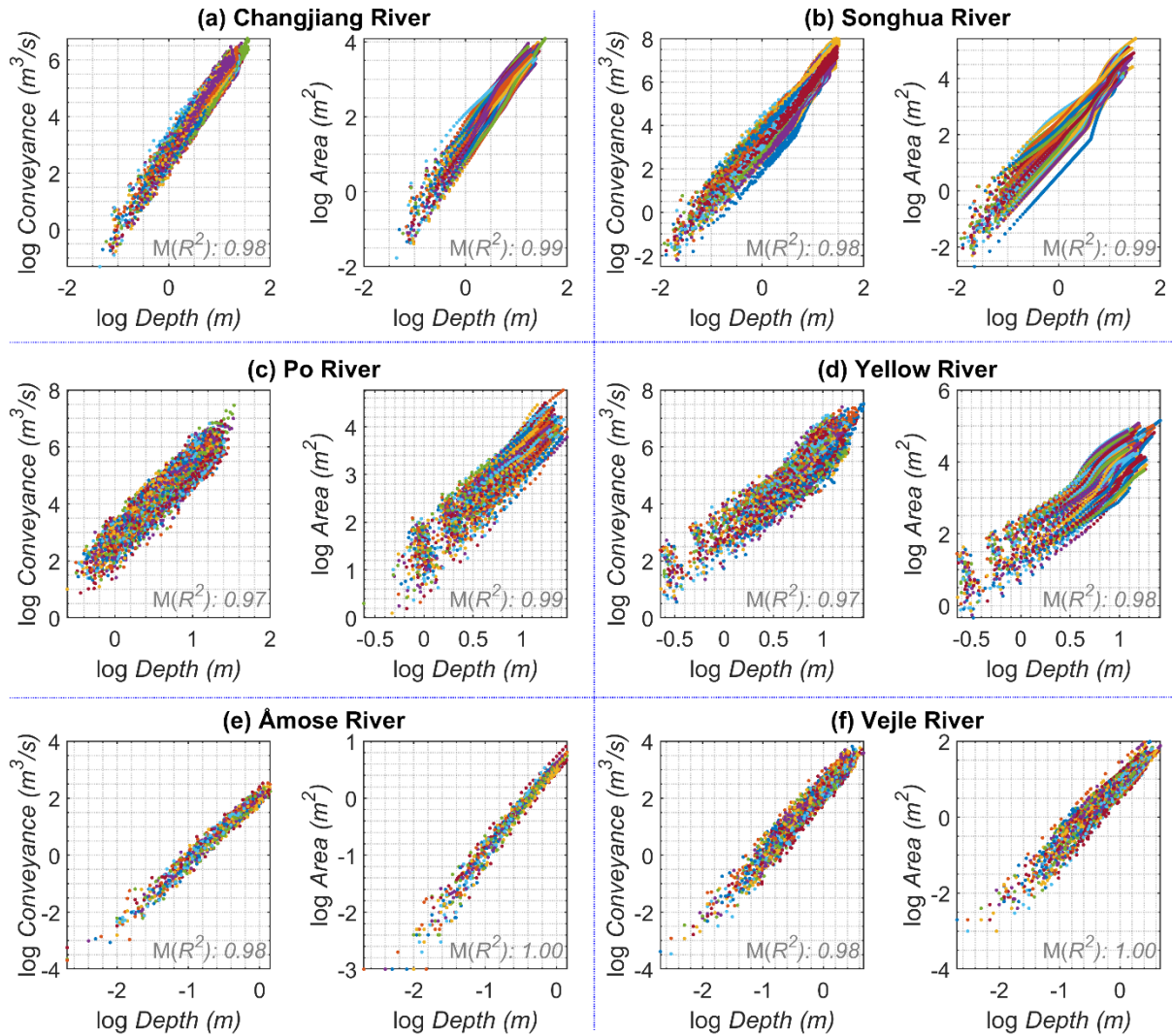


**Figure 1.** Plots of flow area and conveyance against flow depth in log-log space. In each plot, dots in the same color are from one certain cross section. Linear relationships between logarithmic area / conveyance and depth are estimated for each cross section, i.e. in an “at-a-station” manner. The median value of slopes of linear regression is given in each plot. In total, there are 60, 70, 335, 98, 51, 165 cross sections spaced at 2.5 km, 6 km, 1 km, 8 km, 150 m and 300 m, respectively, for (a) Changjiang, (b) Songhua, (c) Po, (d) Yellow, (e) Åmose, and (f) Vejle rivers. Please refer to Figure S1 for a detailed map. Note that, Manning’s number used for calculation of conveyance for each cross section is randomly generated between 0.015 and 0.05.

120 However, there are four more parameters (i.e.  $\alpha$ ,  $\beta$ ,  $\gamma$ ,  $\delta$ ) for each cross section to be estimated. Due to the linear nature of logarithmic pairs of  $(A, d)$  and  $(K, d)$ , a linear relationship can be derived between logarithmic  $A$  and  $K$  as shown in the data (Figure 2). Therefore, the flow area and conveyance curves can be connected by:

$$\alpha = p_1 + p_2\gamma \quad (11)$$



$$\beta = p_3 + p_4 \delta \quad (12)$$

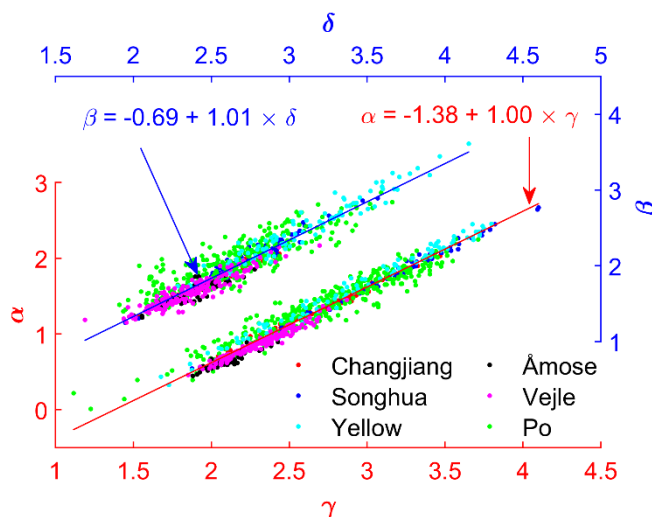
130 It should be noted that the linear relationships (i.e. equations 11 and 12) are only valid at river reach scale instead of individual cross sections. Interestingly,  $p_1$ ,  $p_2$ ,  $p_3$ , and  $p_4$  are nearly constant independent of rivers although marginal deviations exist (Fig. S4). As shown in Figure 2, when pooling cross sections of all rivers together, a clear linear trend shows up for both  $\alpha \sim \gamma$  and  $\beta \sim \delta$ . This indicates that parameters  $p_2$  and  $p_4$  should vary in a very narrow range around 1.0 for all rivers; And parameters  $p_1$  and  $p_3$  should be allowed to be slightly varying around -1.4 and -0.7 to adapt to individual rivers.

135 Thus, there are two spatially varying parameters (i.e.  $\alpha$ ,  $\beta$ ) and four uniform parameters (i.e.  $p_1 \sim p_4$ ) in addition to bed slope  $S_o$  (calculated from datum  $Z_0$ ) to be constrained in order to solve  $Q$  and  $d$ . Therefore, a new parameterization of a river model can be written as:

$$\log_{10}(K(x, t)) = \gamma(x) + \delta(x) \log_{10}(d(x, t)) \quad (13)$$

$$\log_{10}(A(x, t)) = (p_1 + p_2 \gamma(x)) + (p_3 + p_4 \delta(x)) \log_{10}(d(x, t)) \quad (14)$$

140 with  $p_1$ ,  $p_2$ ,  $p_3$ , and  $p_4$ , close to -1.4, -0.7, 1.0 and 1.0, respectively.



145 **Figure 2.** Linear relationship between alpha/beta and gamma/delta. Each dot represents one cross section of a certain river. Dots of the same color are from the same river. Manning's number for each cross section is randomly generated between 0.015 and 0.05. Note that, the best-fit line for each river is slightly different. The relationship using a uniform Manning's number of 0.03 is also given in Figure S3. Individual fitting lines are shown in Figure S4.

### 2.3 Parameter calibration

Hydraulic parameter calibration is essentially an inverse problem that is often solved using the least squares approach. In this study, a non-linear least-squares solver, i.e. the Levenberg-Marquardt algorithm, is used to solve the calibration problem by



150 minimizing the objective function. An ensemble of 10 calibrations with different starting models are conducted to avoid local minima.

Considering the large number of parameters ( $p_1$ ,  $p_2$ ,  $p_3$ , and  $p_4$ , and spatially varying  $Z_0$ ,  $\gamma$  and  $\delta$ ), regularization is used to stabilize the ill-posed problem (Pereverzyev et al., 2006; Schmidt, 2005). In this work, the Tikhonov type regularization is applied and the objective function is formulated following (Aster et al., 2018):

$$\min_{\mathbf{X}} \varnothing(x) = \min_{\mathbf{X}} (\|r(\mathbf{X})\|_2^2 + \lambda^2 \|\mathbf{L}\mathbf{X}\|_2^2) \quad (15)$$

155 where  $\mathbf{X}$  is vector containing the parameters described above;  $r(\mathbf{X})$  is the residuals between model predictions and observations (i.e. water level and width);  $\lambda^2$  is the regularization parameter that controls the strength of the regularization; and  $\mathbf{L}$  is a roughening matrix that constrains the model space. In this study, the first-order regularization is used to smooth the model space. It is a finite difference approximation to the first derivative of the model. The larger  $\lambda$  is, the smoother the model parameters are. For detailed objective function and model calibration, please refer to the supporting information (Text  
160 S2).

Essentially, by optimizing Eq. (15) using satellite derived observations of WSE and river width, we calibrate the two curves, i.e., the relationships between flow area / conveyance and depth as described by equations (13) and (14).

### 3 Case study

To test whether this approach is able to reproduce realistic flow area and conveyance curves as well as WSE using remote  
165 sensing data, we use the Songhua River as a test site (Figure S5). It is the longest tributary of the Amur (or Heilong Jiang), and somewhat representative of large rivers worldwide. It allows testing the approach using satellite data sets, such as altimetry and imagery, which will be available simultaneously from the future SWOT mission (Biancamaria et al., 2016). We use the same reach (433 km evenly divided by 23 cross sections) and boundary conditions as used in Jiang et al. (2019). Specifically, observed discharge is used as the upstream boundary while normal depth is set as downstream boundary.  
170 Inflows of three tributaries are from gauging records while remaining tributary inflows are simulations from a hydrological model (Jiang et al., 2019). The only available in-situ surveyed cross sections are from the late 1990s. These “real” area curves are only used as a benchmark for the calibration results. The validation is focused on the reproduction of WSE at two independent gauging stations as well as altimetry virtual stations. Currently, satellite altimetry derived WSE and satellite imagery derived river width are widely used data sets to study river dynamics (Alsdorf et al., 2007). Therefore, the  
175 calibration data sets used are WSE and water surface width, which are derived from CryoSat-2 altimetry and Landsat imagery, respectively. CryoSat-2 observations are the same as those used in Jiang et al. (2019) while widths are processed using the RivWidthCloud algorithm in Google Earth Engine (Yang et al., 2020). The experiments are conducted under several scenarios to test the capability of different data sets, i.e. WSE only, width only, and both WSE and width combined

(see Text S3 for further explanation). Spatio-temporal distribution of both data sets is shown in Fig. S6. We use the MIKE

180 Hydro River model to implement this approach (see Text S2 for more details).

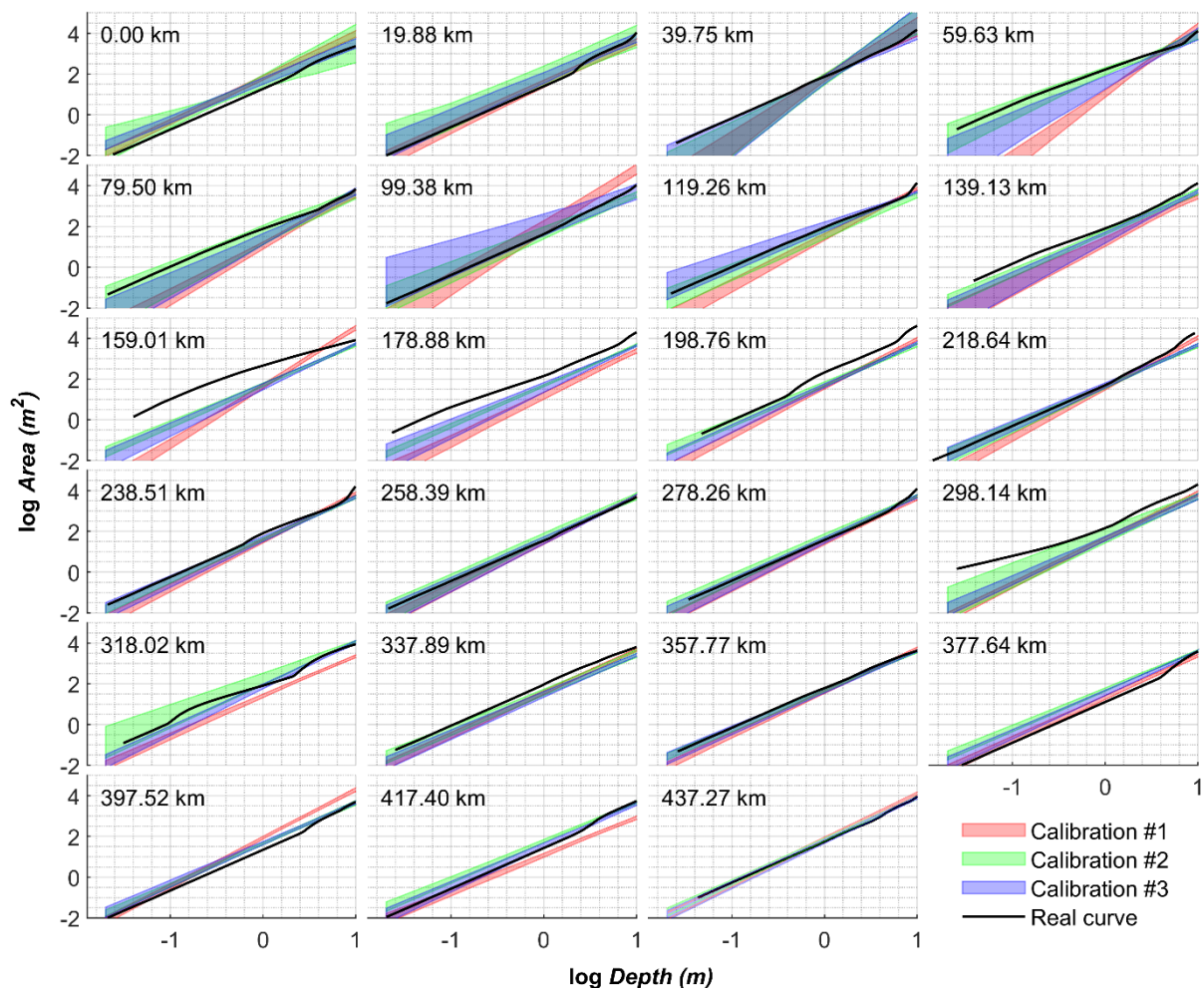


**Figure 3.** Calibrated area-depth curves at 23 cross sections (chainage is given in each plot). Three scenarios are shown, i.e. calibration with water surface elevation data only (calibration #1), river width only (calibration #2), and both water surface elevation and width (calibration #3), respectively. The color band represents the mean  $\pm$  standard deviation based on an ensemble of 10 calibrations.

185

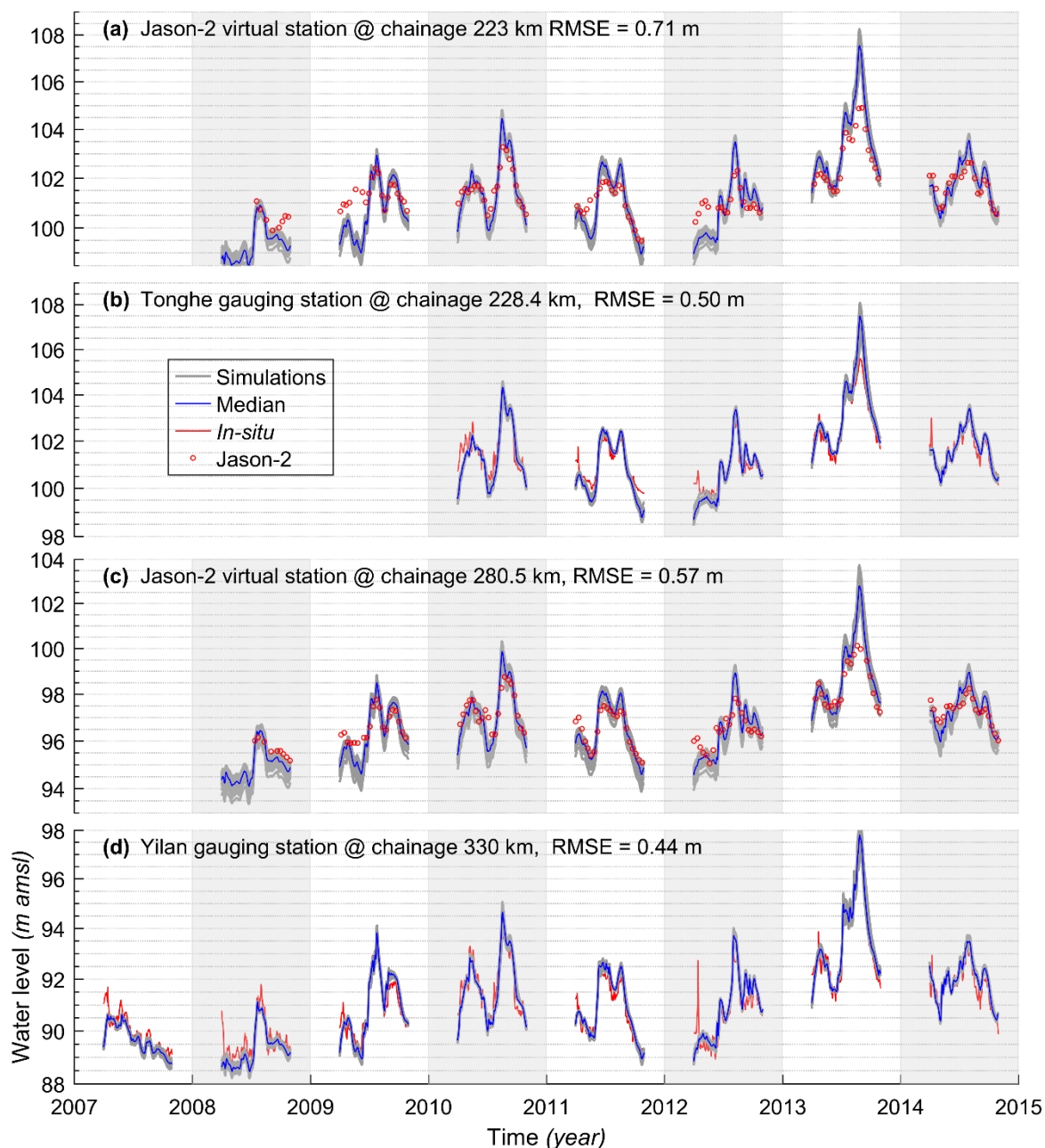
Results prove the feasibility of calibration of spatially varying area-depth curves using solely satellite data sets. Figure 4 depicts the calibrated area-depth curves at 23 cross sections under the three scenarios. Compared to the curves derived from surveyed cross sections, calibrated ones are reasonably close at most locations. Interestingly, either WSE or river width is able to constrain the model to a certain degree (Figure 3), and calibrated model can reproduce WSE with similar RMSE at two gauging stations (see Fig. S7). However, calibration #2 (width only) has larger spread; calibration #3 (both WSE and width) shows the best match with the observed cross sections (Figure 3). Moreover, very dense observations of width (one

190





per 30 m) do not improve the calibration result compared to less dense one (one per 5 km, Fig. S8) although high-resolution imagery (30 m) can provide plenty of width observations. It should be noted that the reservoir in the upstream portion (chainage 20 - 90 km) is not modelled, which explains the large uncertainty of the curves in the upstream.



195

**Figure 4.** Validation of simulated water level (non-frozen periods) at four stations. (a) and (c) are water levels at two virtual stations, i.e. data derived from Jason-2 altimetry. (b) and (d) are from two stream gauging stations. Note, in each plot, results



of the median and individual simulations of an ensemble of 30 calibrations (three scenarios of width observations, see Text S3) are shown.

200 The calibrated model can reproduce WSE reasonably well compared with independent data sets. Figure 4 shows simulated WSE using calibrated curves shown in Figure 3. Overall, the accuracy of simulation is acceptable and comparable to what was achieved using a different approach (Jiang et al., 2019). A careful comparison indicates that the simulations are slightly better than those reported in Jiang et al. (2019), especially for low WSE. Compared to Yilan, Tonghe shows slightly higher RMSE (Figure 4) due to the underestimation of extremely high WSE in 2013, although the simulated discharge  
205 matches in situ observations well (Figure S9). This can be well explained by the calibrated curves. The curves at two neighboring cross sections (chainage 218.64 and 238.51 km) show deviations from the curves derived from surveyed cross sections beyond bankfull depth. Evaluation at two virtual stations also shows good agreements. However, model simulation is better than Jason-2 observations except during the 2013 flood by referring to the hydrograph of adjacent gauging stations (Figure 4).

#### 210 4 Discussion

For our case study, models calibrated with either river width or WSE show similar performance in terms of RMSE of WSE at two gauging stations (Fig. S7). However, both cases have problems to fully constrain models and suffer from model ambiguity, which means parameters cannot be well determined. A direct consequence is that model simulation of either the WSE or river width is not physically meaningful (Fig. S10). Because both cases can achieve a reasonable area-depth  
215 relationship by making a trade-off between datum and WSE or river width. Therefore, both WSE and river width are needed to better constrain model parameters.

Nevertheless, river width and WSE may play different roles in constraining parameters for different rivers depending on the channel shape. If a channel is embanked, for instance, model parameters may not be sensitive to the small changes of river width. This issue certainly needs further investigation. Obviously, observations of river width are easier to obtain and  
220 have higher frequency and larger coverage than altimetry-derived WSE (usually the frequency is lower than 10 days). That is, this approach can be applied in many rivers where altimetry data is also available given reliable discharge as the upstream boundary. This raises a question: Can area and conveyance curves be estimated using short-repeat altimetry missions, such as Jason or Sentinel-3? Our previous study (Jiang et al., 2019) shows that spatial sampling density is more important than temporal frequency in the context of hydraulic inversion and that Jason series alone are not able to constrain the spatially  
225 distributed parameters. The trade-off between spatial and temporal sampling density in inland radar altimetry merits further investigation. Moreover, rapid advances in drone technology also provide WSE and width for small rivers (Bandini et al., 2020). Therefore, this approach is also applicable to rivers where satellite altimetry data are not available.



The new parameterization proposed in this paper can also be used with simulated discharge instead of observed discharge. We performed a preliminary investigation on the effect of simulated discharge errors on inverted area and conveyance curves. Specifically, for the upstream boundary, modelled discharge from a regional rainfall-runoff model is used instead of in-situ discharge (Fig. S11). With this setup, the calibrated 1-D hydrodynamic model can reproduce WSE reasonably well (~0.9 m, see Fig. S11). The accuracy is comparable to previous studies, such as Domeneghetti et al. (2014) although surveyed cross sections were used in those studies. This finding demonstrates that this approach has great potential to be applied in ungauged river basins.

As we mentioned, this study only focuses on the main channel and does not account for overbank flow. In the presence of significant floodplains, the linearity of the curve may fail at bankfull depth as seen in Figure 1 and 3. To solve this problem, a second curve is needed to describe the overbank flow as suggested by Garbrecht (1990). On the other hand, instead of calibrating the second curve, real data (such as high resolution DEMs, or ICESat-2, etc.) of the non-inundated portion can be used to parameterize the curves.

This approach opens up a range of possibilities to simulate and predict flow dynamics in data scarce regions. In addition to simulating WSE as illustrated in previous sections, discharge retrieval is also possible once the slope is known based on established conveyance curves. The future SWOT mission will deliver WSE and slope simultaneously, which can support discharge retrieval using this approach.

## 5 Conclusions

Directly calibrating roughness and cross-sectional geometry of river models is still challenging. In this paper, we propose a new parameterization method to calibrate 1-D hydrodynamic river models using altimetry and imagery observations. The workflow is based on the power-law relationships between flow area / conveyance and flow depth, which is not new and has been described half a century ago (Chow, 1959). In this study, we discovered that the two curves are very well correlated, and the relationship is generally independent of rivers. The novelty of this study is that the flow area and conveyance can be inverted directly using spatially distributed observations of WSE and river width given the boundary conditions. In this way, no explicit considerations of roughness and channel geometry are needed to solve for WSE.

Our case study demonstrates that the curves can be estimated using solely remote sensing data, and the calibrated hydrodynamic model can reproduce WSE with fairly high precision. Further exploration indicates that this approach can be integrated into a hydrologic-hydrodynamic model for studying ungauged river basins.

Current satellite imagery (Landsat, Sentinel, Gaofen, etc.) and altimetry (CryoSat-2, AltiKa-DF) can support this approach for relatively large rivers. This new parameterization may prove especially useful for poorly gauged rivers when high resolution data sets are available from the upcoming SWOT mission.



**Code and data availability.** River widths were processed on the Google Earth Engine platform. CryoSat-2 were from the study of Jiang et al. (2019). Jason-2 data were downloaded from AVISO+ (<https://www.aviso.altimetry.fr/en/data/data-access/ftp.html>). Cross-sectional data of the Changjiang, Songhua, and Yellow rivers were excerpted from the Hydrological Yearbook issued by the Ministry of Water Resources, China. Cross-sectional data of the Po river are publicly available from the Interregional agency for the river Po ([http://geoportale.agenziapo.it/web/index.php/it/?option=com\\_aipograf3](http://geoportale.agenziapo.it/web/index.php/it/?option=com_aipograf3)). Data of the Danish rivers (Åmose, Vejle) were kindly provided by WSP (<http://www.hydrometri.dk/hyd/>).

**Author contributions.** SWC developed the methodology in an early stage with inputs from LJ and PBG. LJ further developed the methodology, did the data curation, and performed the calibration work. LG prepared the manuscript. All authors contributed to editing the manuscript.

**Competing interests.** The authors declare that they have no conflict of interest.

**Acknowledgements.** The authors would like to thank AVISO+, WSP and AIPo for making the data sets available.

**Financial support.** This work is jointly funded by the Danida Fellowship Centre (File number: 18-M01-DTU) and the Innovation Fund Denmark (File number: 8087-00002B).

## References

- Andreadis, K. M. and Schumann, G. J. P.: Estimating the impact of satellite observations on the predictability of large-scale hydraulic models, *Adv. Water Resour.*, 73, 44–54, doi:10.1016/j.advwatres.2014.06.006, 2014.
- Annis, A., Nardi, F., Volpi, E. and Fiori, A.: Quantifying the relative impact of hydrological and hydraulic modelling parameterizations on uncertainty of inundation maps, *Hydrol. Sci. J.*, 65(4), 507–523, doi:10.1080/02626667.2019.1709640, 2020.
- Bates, P. D., Neal, J. C., Alsdorf, D. and Schumann, G. J.-P.: Observing Global Surface Water Flood Dynamics, *Surv. Geophys.*, 35(3), 839–852, doi:10.1007/s10712-013-9269-4, 2014.
- Bierkens, M. F. P.: Global hydrology 2015: State, trends, and directions, *Water Resour. Res.*, 51(7), 4923–4947, doi:10.1002/2015WR017173, 2015.
- Blöschl, G., Gaál, L., Hall, J., Kiss, A., Komma, J., Nester, T., Parajka, J., Perdigão, R. A. P., Plavcová, L., Rogger, M.,



- Salinas, J. L. and Viglione, A.: Increasing river floods: fiction or reality?, *Wiley Interdiscip. Rev. Water*, 2(4), 329–344,  
285 doi:10.1002/wat2.1079, 2015.
- Brisset, P., Monnier, J., Garambois, P.-A. and Roux, H.: On the assimilation of altimetric data in 1D Saint–Venant river flow  
models, *Adv. Water Resour.*, 119, 41–59, doi:10.1016/j.advwatres.2018.06.004, 2018.
- Dey, S., Saksena, S. and Merwade, V.: Assessing the effect of different bathymetric models on hydraulic simulation of rivers  
in data sparse regions, *J. Hydrol.*, 575(March), 838–851, doi:10.1016/j.jhydrol.2019.05.085, 2019.
- 290 DHI: MIKE HYDRO River - User Guide, DHI, Copenhagen., 2017.
- Dingman, S. L.: Analytical derivation of at-a-station hydraulic–geometry relations, *J. Hydrol.*, 334(1–2), 17–27,  
doi:10.1016/j.jhydrol.2006.09.021, 2007.
- Domeneghetti, A.: On the use of SRTM and altimetry data for flood modeling in data-sparse regions, *Water Resour. Res.*,  
52(4), 2901–2918, doi:10.1002/2015WR017967, 2016.
- 295 Durand, M., Andreadis, K. M., Alsdorf, D. E., Lettenmaier, D. P., Moller, D. and Wilson, M.: Estimation of bathymetric  
depth and slope from data assimilation of swath altimetry into a hydrodynamic model, *Geophys. Res. Lett.*, 35(20), L20401,  
doi:10.1029/2008GL034150, 2008.
- Fleischmann, A., Paiva, R. and Collischonn, W.: Can regional to continental river hydrodynamic models be locally relevant?  
A cross-scale comparison, *J. Hydrol. X*, 3, 100027, doi:10.1016/j.hydroa.2019.100027, 2019.
- 300 Fonstad, M. A. and Marcus, W. A.: Remote sensing of stream depths with hydraulically assisted bathymetry (HAB) models,  
*Geomorphology*, 72(1–4), 320–339, doi:10.1016/j.geomorph.2005.06.005, 2005.
- Garambois, P.-A., Calmant, S., Roux, H., Paris, A., Monnier, J., Finaud-Guyot, P., Samine Montazem, A. and Santos da  
Silva, J.: Hydraulic visibility: Using satellite altimetry to parameterize a hydraulic model of an ungauged reach of a braided  
river, *Hydrol. Process.*, 31(4), 756–767, doi:10.1002/hyp.11033, 2017.
- 305 Garambois, P. A. and Monnier, J.: Inference of effective river properties from remotely sensed observations of water surface,  
*Adv. Water Resour.*, 79, 103–120, doi:10.1016/j.advwatres.2015.02.007, 2015.
- Gleason, C. J. and Durand, M. T.: Remote Sensing of River Discharge: A Review and a Framing for the Discipline, *Remote  
Sens.*, 12(7), 1107, doi:10.3390/rs12071107, 2020.
- Grimaldi, S., Li, Y., Walker, J. P. and Pauwels, V. R. N.: Effective Representation of River Geometry in Hydraulic Flood  
310 Forecast Models, *Water Resour. Res.*, doi:10.1002/2017WR021765, 2018.
- Jiang, L., Madsen, H. and Bauer-Gottwein, P.: Simultaneous calibration of multiple hydrodynamic model parameters using  
satellite altimetry observations of water surface elevation in the Songhua River, *Remote Sens. Environ.*, 225, 229–247,  
doi:10.1016/j.rse.2019.03.014, 2019.
- Jiang, L., Bandini, F., Smith, O., Klint Jensen, I. and Bauer-Gottwein, P.: The Value of Distributed High-Resolution UAV-  
315 Borne Observations of Water Surface Elevation for River Management and Hydrodynamic Modeling, *Remote Sens.*, 12(7),  
1171, doi:10.3390/rs12071171, 2020.
- Larnier, K., Monnier, J., Garambois, P. A. and Verley, J.: River discharge and bathymetry estimation from SWOT altimetry



- measurements, *Inverse Probl. Sci. Eng.*, doi:10.1080/17415977.2020.1803858, 2020.
- Legleiter, C. J.: Calibrating remotely sensed river bathymetry in the absence of field measurements: Flow REsistance  
320 Equation-Based Imaging of River Depths (FREEBIRD), *Water Resour. Res.*, 51(4), 2865–2884,  
doi:10.1002/2014WR016624, 2015.
- Mejia, A. I. and Reed, S. M.: Evaluating the effects of parameterized cross section shapes and simplified routing with a  
coupled distributed hydrologic and hydraulic model, *J. Hydrol.*, 409(1–2), 512–524, doi:10.1016/j.jhydrol.2011.08.050,  
2011.
- 325 Mersel, M. K., Smith, L. C., Andreadis, K. M. and Durand, M. T.: Estimation of river depth from remotely sensed hydraulic  
relationships, *Water Resour. Res.*, 49(6), 3165–3179, doi:10.1002/wrcr.20176, 2013.
- Moramarco, T., Barbeta, S., Bjerklie, D. M., Fulton, J. W. and Tarpanelli, A.: River Bathymetry Estimate and Discharge  
Assessment from Remote Sensing, *Water Resour. Res.*, 55(8), 6692–6711, doi:10.1029/2018WR024220, 2019.
- Neal, J., Schumann, G. and Bates, P.: A subgrid channel model for simulating river hydraulics and floodplain inundation  
330 over large and data sparse areas, *Water Resour. Res.*, 48(11), 1–16, doi:10.1029/2012WR012514, 2012.
- Neal, J. C., Odoni, N. A., Trigg, M. A., Freer, J. E., Garcia-pintado, J., Mason, D. C., Wood, M. and Bates, P. D.: Efficient  
incorporation of channel cross-section geometry uncertainty into regional and global scale flood inundation models, *J.  
Hydrol.*, 529, 169–183, doi:10.1016/j.jhydrol.2015.07.026, 2015.
- Pappenberger, F., Beven, K., Frodsham, K., Romanowicz, R. and Matgen, P.: Grasping the unavoidable subjectivity in  
335 calibration of flood inundation models: A vulnerability weighted approach, *J. Hydrol.*, 333(2–4), 275–287,  
doi:10.1016/j.jhydrol.2006.08.017, 2007.
- Schaperow, J. R., Li, D., Margulis, S. A. and Lettenmaier, D. P.: A Curve-Fitting Method for Estimating Bathymetry From  
Water Surface Height and Width, *Water Resour. Res.*, 55(5), 4288–4303, doi:10.1029/2019WR024938, 2019.
- Schneider, R., Godiksen, P. N., Villadsen, H., Madsen, H. and Bauer-Gottwein, P.: Application of CryoSat-2 altimetry data  
340 for river analysis and modelling, *Hydrol. Earth Syst. Sci.*, 21(2), 751–764, doi:10.5194/hess-21-751-2017, 2017.
- Schumann, G., Matgen, P., Hoffmann, L., Hostache, R., Pappenberger, F. and Pfister, L.: Deriving distributed roughness  
values from satellite radar data for flood inundation modelling, *J. Hydrol.*, 344(1–2), 96–111,  
doi:10.1016/j.jhydrol.2007.06.024, 2007.
- Ward, P. J., Jongman, B., Salamon, P., Simpson, A., Bates, P., De Groeve, T., Muis, S., de Perez, E. C., Rudari, R., Trigg,  
345 M. A. and Winsemius, H. C.: Usefulness and limitations of global flood risk models, *Nat. Clim. Chang.*, 5(8), 712–715,  
doi:10.1038/nclimate2742, 2015.